

Title

High-resolution genetic maps identify multiple type 2 diabetes loci at regulatory hotspots in African Americans and Europeans

Authors:

Winston Lau¹, Toby Andrew^{2*}, Nikolas Maniatis^{1*}

¹Department of Genetics, Evolution and Environment, University College London, WC1E 6BT London, UK; ²Department of Genomics of Common Disease, Imperial College London, W12 0NN London, UK

*Equal authorship

Corresponding author: Nikolas Maniatis

ABSTRACT

Interpretation of results from genome-wide association studies for T2D is challenging. Only very few loci have been replicated in African ancestry populations and the identification of the implicated functional genes remain largely undefined.

We used genetic maps that capture detailed linkage disequilibrium information in European and African-Americans and applied these to large T2D case-control samples in order to estimate locations for putative functional variants in both populations. Replicated T2D locations were tested for evidence of being regulatory hotspots using adipose expression. We validated a sample of our co-location intervals using next generation sequencing and functional annotation, including enhancers, transcription and chromatin modifications.

We identified 111 additional disease-susceptibility locations, 93 of which are cosmopolitan and 18 are European specific. We show that many previously known signals are also risk loci in African-Americans. The majority of the disease locations appear to confer risk of T2D via the regulation of expression levels for a large number (266) of *cis*-regulated genes, the majority of which are not the nearest genes to the disease loci. Sequencing three cosmopolitan locations provided candidate functional variants that precisely co-locate with cell-specific chromatin domains and pancreatic islet enhancers. These variants have large effect sizes and are common across populations.

Results show that disease-associated loci in different populations, gene expression and cell-specific regulatory annotation can be effectively integrated by localizing these effects on high-resolution genetic maps. The *cis*-regulated genes provide insights into the complex molecular pathways involved and can be used as targets for sequencing and functional molecular studies.

INTRODUCTION

No disease with a genetic predisposition has been more intensely investigated than Type 2 diabetes (T2D [MIM: 125853]), the world's most widespread and devastating metabolic disorder. Over the last 10 years, numerous consortia have undertaken to characterize the genetic causes of T2D through a very large number (>30) of genome-wide association studies (GWAS), and large-scale meta-analyses. Initially based on Europeans, the focus has now shifted to the replication of risk loci in additional ethnicities (trans-ethnic studies), motivated in part by the likely wider application of cosmopolitan variants for translational research, but also the desire for increasingly larger research sample sizes in order to try to boost study power¹. But since T2D is really a group of diseases², increased sample size should be met with scepticism unless accompanied by more detailed clinical phenotypes and strategies to minimise disease heterogeneity. Recent trans-ethnic meta-analysis of T2D for four populations (Europeans, East Asians, South Asians and Mexican Americans) has identified seven T2D loci³, in addition to the previously published list of 69 loci⁴. However, a large proportion of these 76 loci³ do not show evidence for nominal association for the same 'lead' SNP. Since the lead SNP is unlikely to be the causal variant, this low replication rate is a general problem for trans-ethnic studies⁵. The inability to account for genetic distance between neighbouring SNPs and genetic heterogeneity (e.g. locus and allele heterogeneity and variation in LD between populations) are both potential thwarting factors in the endeavour to identify trans-ethnic disease loci.

On the other hand, the prevalence of T2D in African-Americans (19%) at approximately twice that of European Americans (10%), and the existence of more genetic diversity in peoples of African ancestry, partly due to less extensive linkage disequilibrium (LD), also gives rise to a major opportunity for comparative fine mapping studies^{3; 6; 7}. This possibility was missed by a recent major trans-ethnic meta-analysis that unfortunately excluded African-Americans³. Here we seek to take advantage of this ancestry group by using a mapping approach to identify cosmopolitan T2D locations, which avoids the focus on lead SNPs. Instead we use high-resolution genetic maps to identify new cosmopolitan T2D susceptibility loci that are shared by both European and African-American populations. Genetic distances from these maps accurately capture the genetic architecture of the relevant population and have been successfully used in gene mapping studies for other common diseases^{8; 9}. We constructed genetic maps for each of these two populations and then used disease-associated location estimates on these maps as the basis for the precise co-localization and replication in both populations. We also analysed all 76 previously known T2D loci³ to obtain refined location estimates on the same genetic maps. Since an estimated 90% of variants with a functional role in complex traits such as T2D are likely to be non-coding and regulatory¹⁰, we assessed this scenario by exploiting publicly available subcutaneous adipose expression data. The hypothesis we tested is that T2D disease loci confer risk of disease by acting as expression quantitative trait loci (eQTL) that regulate the expression of neighbouring (*cis*-) genes. To test this hypothesis, we used the same genetic maps to assess whether the location estimates for eQTL also precisely collocated with those mapped for T2D in this whole-genome analysis, thereby identifying potential *cis*-genes and pathways regulated by the disease loci. Finally, we performed fine

mapping using targeted next generation sequencing (NGS) of the refined location estimates for one previously known locus (*TCFL72*) and two of the additional cosmopolitan loci from this study using independent case/control sample data, with the aim of identifying the candidate functional variants at the causal location estimates. These examples illustrate a way forward for the systematic identification of putative functional variants at these identified disease-associated eQTLs, coupled with the integration of functional annotation such as cell-specific chromatin domain modifications, enhancers and transcription binding sites.

METHODS

STUDY DESIGN

We analysed two European (EUR) and one African-American (AA) samples with a total of 5,800 T2D cases and 9,691 controls. The two independent EUR samples (SNP-arrays for GWA and Metabochip) were obtained from the Wellcome Trust Case Control Consortium (WTCCC)^{11; 12} with a description of diagnostic criteria and sample matching provided in Supplementary Materials. The AA GWA sample for a population of predominantly African ancestry was obtained from the National Institute of Diabetes and Digestive and Kidney Diseases (NIDDK)¹³. Analysing “one-SNP-at-a-time” ignores LD structure when testing for association with disease or gene expression. Here we use population-specific genetic maps, which provide (i) commensurability when making comparisons between different populations and SNP arrays; (ii) the means to implement a multi-marker test of association¹⁴; (iii) genetic distances between loci when testing for association with disease or adipose expression; and (iv) precise location estimates on the genetic map for potential functional variants, since these estimates are more efficient than using physical maps¹⁵. We constructed two high-resolution genetic maps based upon HapMap data with genetic distances expressed in LD units (LDU)¹⁶. The EUR LDU map was used for analyses of the two EUR T2D datasets and the AA LDU map was used for the analysis of the AA T2D dataset. The autosomal genome (sex chromosomes were not included in the analyses) was divided into 4,800 non-overlapping analytical windows with a minimum LDU distance of 10 LDU. In addition to windows being the same minimum size on the genetic map, each window also had to include a minimum of 30 SNPs. These

criteria yielded an average genetic length of 11 LDU. The identical boundaries in kilobases (kb) for all 4,800 analytical windows were used for the AA dataset, but with longer average genetic length (16 LDU), reflecting a population history of greater antiquity with additional historical recombination events. All SNPs in each analytical window were simultaneously used to test for association with disease using a multi-marker LDU model¹⁴. The analysis returns one estimated location for a causal variant with the strongest signal, along with the association test *P*-value for each window. Utilizing the genetic map in this way, the multi-marker test of association models the degree of regional LD when estimating the location of a putative causal variant on the genetic map. A schematic diagram of the functional genomic strategy used in the current study is provided in Figure 1. Strict criteria were used for the meta-analysis. Location estimates for genome-wide significant meta-analysis loci had to be nominally significant in both ancestry groups for the cosmopolitan loci and in both European samples for the European-specific loci. An interval criterion was used where location estimates from different datasets had to be within <100 kb of one another to qualify as a potential replication. Replicated loci had to pass a Bonferroni corrected meta-analysis *P*-value threshold of 1×10^{-5} , based on the total number of genomic tests performed ($\alpha=0.05/4,800$). We refer to the co-location interval (distance between location estimates) as the genomic region that most plausibly include the functional variants that confer risk of T2D.

We conducted *in silico* functional gene expression analyses to assess whether the same T2D loci are also eQTL that regulate the expression of neighbouring *cis*-genes using data generated by the MuTHER consortium¹⁷. Summary statistics for the probes and SNPs are

available from the MuTHER website. Using adipose tissue mRNA expression probes as quantitative traits; we tested for *cis*-association at each disease locus by employing the same multi-locus LDU model, with potential regulated *cis*-genes defined to be within ± 1.5 Mb distance either side of each replicated T2D causal locations (Figure 1). We only considered a disease locus to be a potential eQTL, if the estimated eQTL co-located to within 50 kb of the T2D location and passed Bonferroni correction for the total number of probes tested within ± 1.5 Mb of each replicated disease locus. All LDU location estimates for both T2D and eQTL on the genetic map were converted back to kb B36 (NCBI36/hg18) for presentational purposes.

Finally, we conducted a NGS targeted re-sequencing experiment for three of the disease loci. Next generation sequencing was conducted using the Agilent SureSelect^{XT2} capture kit following manufacturer protocol guidelines for 100 ng of DNA. Blood DNA samples were sequenced for a total of 94 unrelated European individuals with T2D and 94 unaffected controls 1:1 matched for age, BMI and sex. Cases with a family history of T2D (selection and diagnosis criteria described elsewhere)¹⁸ and controls were selected from families originally collected for an obesity (MIM: 601665) study without a history of T2D¹⁹. Additional method details are provided in the supplementary material.

RESULTS

ADDITIONAL LOCI FOR T2D

Tables 1 and 2 present the results for the 111 additional loci associated with T2D. Of the 111 loci, 93 provide evidence of being cosmopolitan (signals 1–93, Table 1), since these loci replicate for both EUR and AA samples, while 18 loci appear to be European-specific (94–111, Table 2), with replication in European samples only. The distances between T2D location estimates for the majority of the 111 loci were narrow (<50kb apart). Estimation of average pairwise D-prime (D') for all HapMap SNPs found within all the identified 111 disease location intervals (ranging from 0 to <100kb) is $D'=0.86$ in Europeans and $D'=0.78$ in the AA, which reflect the importance of using a genetic map in LDU distances for localisation and the <100kb interval as a criterion for replication. For the majority of the cosmopolitan loci (signals 6–80, Table 1) the MetaboChip array was not informative due to the very low SNP coverage in many regions (symbol ‘-’ in Table 1). Some signals for MetaboChip passed the minimal number of SNPs (>30 per window), but did not provide significant evidence of association (‘ns’ in Table 1) due to the uneven genomic coverage of SNPs on the customized MetaboChip design¹². For this reason, there were only 13 cosmopolitan loci (signals 81–93, Table 1) that provided replicated evidence for AA and MetaboChip European samples.

For the 111 additional T2D loci, half of the location estimates are intragenic and half are intergenic. For the latter, we follow the convention of labeling the disease loci using the nearest gene symbol (within 100kb from the T2D location). The *in silico* expression

analyses, however, indicate which *cis*-genes are regulated and therefore functionally implicated by the identified T2D loci. Two-thirds (71/111) of the disease loci also show strong evidence of being eQTLs using our stringent criteria but the remaining one-third may well reflect that these replicated loci could be eQTLs for a T2D-relevant tissue other than subcutaneous adipose. The 71 eQTL signals regulate the expression of a conservatively estimated total of 183 *cis*-genes (Tables 1 and 2), the majority of which are not genes that are the nearest to the disease locus. Indeed, further investigation of the 183 *cis*-genes substantiates quantitatively what has previously been suspected. Namely, that the physical kb distance of the eQTL to the *nearest* gene (Figure 1) is entirely unrelated ($P>0.05$) to the distance between the same eQTL and the actual (*cis*-associated) *functional* gene (see supplementary Figure S1). This result demonstrates that the assumption that the nearest gene is also the most likely candidate functional gene is not justified. Further analysis of the 183 *cis*-genes also showed that the distance between the eQTL and the T2D location estimates is not biased by the distance between the T2D sample location estimates within the <100kb interval (see supplementary Figure S2).

Interestingly, approximately 40% of the eQTL signals observed in this study have at least one *cis*-gene previously known as one whose expression (in adipose or liver) is also strongly associated with BMI in morbidly obese individuals²⁰. We also show that a number of the identified T2D loci also regulate the expression levels of nuclear encoded mitochondrial genes. For example, many *cis*-genes implicate T2D through the regulation of the molecular functions of fatty acid metabolism (*PCCA* [MIM: 232000], *ACAD11* [MIM: 614288], signals 66 and 99, respectively); glycerophospholipid metabolism (*PISD*

[MIM: 612770], *GPAM* [MIM: 602395], signals 80 and 117); pyruvate metabolism (*PDHA2* [MIM: 179061], *HAGH* [MIM: 138760], signals 26/27 and 68); mitochondrial transcription and translation (*MTERFD3* [MIM: 616929], *LACTB* [MIM: 608440], *TRMT11* [MIM: 609752], signals 61, 90, 105); and mitochondrial protein transport (*GFER* [MIM: 600924], signal 68). The *cis*-genes *PDHA2* and *PCCA* (signals 26/27 and 66, respectively) directly implicate the genetic dysregulation of Krebs cycle function as a risk factor for T2D.

To further characterize the observed T2D and associated eQTL location estimates in relation to potential functional variants, three of the cosmopolitan loci were targeted for sequencing using an independent sample of Europeans. Figure 2 presents an example of a regulatory intergenic hotspot near *ACTL7B* [MIM: 604304] on chromosome 9q31.3 (signal 46, Table 1). The two genetic maps (Y-axis in LDU) for AA and EUR are plotted against the physical genomic region (X-axis in kb), with each data point representing a HapMap SNP from which the genetic LDU maps were inferred (Figure 2b). Cumulative LDU plots the non-linear relationship between physical distance and the underlying LD, which is typically a “Block-Step” structure. Blocks of LD (SNPs with the same LDU location) represent areas of conserved LD and low haplotype diversity, while Steps (increasing LDU distances) define LD breakdown, primarily caused by recombination, since crossover profiles agree precisely with the corresponding LDU steps¹⁶. The maps show numerous short blocks across the entire region with total LDU length being greater for AA (greater LD breakdown) than the EUR population. The functional location estimates A and E (13kb apart) indicated by the vertical solid line arrows are associated with T2D in AA and EUR

samples, respectively. The dotted lines, in close proximity to the T2D locations (<30 kb), represent the location of eQTLs that regulate the expression of *KLF4* [MIM: 602253] and *EPB41LAB* [MIM: 610340] in subcutaneous adipose (nine genes reside between the two illustrated, but for clarity only the *cis*-genes regulated by the T2D-associated eQTL are plotted). *KLF4* and *EPB41LAB* are 1.3Mb downstream and 350kb upstream, respectively. Targeted next-generation re-sequencing of the 39 kb region centered on these A and E locations shows evidence of association between T2D and variants, which coincide with the estimates for the T2D-associated eQTL (summary statistics of the NGS SNPs are provided in Figure 2a). Although only nominally significant ($P < 0.05$) due to small sample size (94 cases and 94 controls), these common variants both confirm the expected location estimate and account for a relatively large risk of disease (odds ratio (OR) of 2.0–2.4), with the risk allele frequencies (RAF) being similar in a number of human populations from the 1000 Genomes Project. Examination of the epigenetic chromatin marks from trimethylation of histone H3 at lysine 4 (H3K4me3) and acetylation of histone H3 at lysine 27 (H3K27ac), which highlight regulatory elements such as active promoters and enhancers²¹ has previously been shown to overlap with T2D loci²², but such marks are often cell type-specific²³. Figure 2c plots the $-\log_{10} P$ -values of the chromatin profiles, demonstrating that T2D causal locations also co-localize with chromatin domains for CD14⁺ monocytes and adipose nuclei. The most intense chromatin peaks were observed in CD14⁺ monocytes at the precise eQTL location for *KLF4* and at rs60388922 and rs72756001 SNPs, which reside within the E and A T2D interval. Hence both of these SNPs are good causal candidate variants.

Figure 3 presents the regulatory Potassium channel, subfamily k, member 3 (*KCNK3* [MIM: 603220]) locus (signal 82, Table 1) on chromosome 2p23.3 with identical location estimates for both AA and EUR samples (Fig. 3b). Despite the disease locus residing within *KCNK3*, expression analyses indicate that this locus is not functionally related to this gene, but instead is a *cis*-eQTL that regulates the distant genes *DNMT3A* [MIM: 602769], *ASXL2* [MIM: 612991], *GAREM2*, *OTOF* [MIM: 603681], *CENPA* [MIM: 117139] and *CCDC121*, with *DNMT3A* and *CCDC121* being 1.5Mb and 896kb away from the eQTL, respectively. This is a gene-rich region (57 genes in total), but for clarity only the six identified *cis*-genes have been plotted. Figure 3a presents summary statistics for the variants associated with T2D for a 42kb targeted re-sequencing region. These associated variants (P -value < 0.05) coincide with the promoter region of *KCNK3*, 11kb upstream from the T2D location estimate and account for a high risk of disease (OR=3.5–4.8). The RAF are approximately 0.05 and the results show that these variants are indeed cosmopolitan, since they are common not only in EUR and AA, but also in other human populations (e.g. East and South Asians and Mexican Americans). Using information from the human pancreatic islet regulome²², where sequences targeted by islet transcription factors highlight active enhancers, we observed that the identified T2D location resides within a cluster of such active enhancers. The transcription factor FOXA2-bound sites are also plotted within the kb boundaries of the active enhancer cluster. Chromatin peaks also overlap with the regulatory T2D and eQTL locations for pancreas and liver cell types (Fig. 3c), suggesting evidence for more than one functional mutation within this region. The full interval for the T2D and eQTL locations were not entirely covered by NGS data, but nevertheless, the associated NGS SNPs reside between two active islet enhancers (Fig. 3b).

In contrast to imputation methods that use high-resolution “out-of-sample” marker panels to infer missing SNPs to subsequently test one at a time, LDU analysis uses marker panels to infer high-resolution genetic maps. Subsequently, multi-marker tests of association use genetic distances for SNP arrays placed on those maps to infer the location of disease-associated functional variants. Fine mapping is therefore achieved by inferring fine-scale genetic maps, not by imputing SNPs. It is worth noting in relation to this that using the *KCNK3* locus as an example, the NGS SNPs genotyped for the case control data that were associated with T2D status (Fig. 3a) could not be imputed based on the 1000G data as the reference panel.

FINDINGS AT PREVIOUSLY KNOWN T2D LOCI

Using the same data and analytical methods, we have confirmed disease location estimates for 62 out of 76 previously known loci³ (supplementary Table S1). Of these, about half (33/62) show evidence of being eQTL with the majority regulating *cis*-genes over 1Mb away. In addition, over one third (22/62) of the loci replicate for AA samples, which were previously excluded from trans-ethnic meta-analysis³. We investigated the Transcription factor 7-like 2 (*TCF7L2* [MIM: 602228]) locus (signal 117, supplementary Table S1). Figure 4b plots the T2D locations for EUR and AA and shows that this signal harbours a *cis*-eQTL for the distant *GPAM*. The T2D re-sequence variants we identified, which co-locate to the <30 kb interval between the T2D and eQTL locations, account for a large risk of disease (OR=1.7–2.6). The summary statistics in Figure 4a show that these risk variants are the major allele in all other human populations. The T2D locations for both populations reside within an active enhancer cluster that is targeted by transcription factor FOXA2 (kb

locations of the regulatory elements are plotted on the X-axis). Inferring the likely transcriptional activity by observing the chromatin state, we show that the eQTL, T2D co-locations and NGS SNPs all map precisely to highly significant H3K4me3 and H3K27ac peaks, in particular in adipose cells (Fig. 4c). This illustrates the importance of co-locating within an interval on the genetic map, since it allows for potential allelic heterogeneity.

DISCUSSION

This study provides a comprehensive genomic catalogue of susceptibility loci for T2D in European and African ancestry populations and evidence that the majority of the additional 111 and 62 previously known disease loci are eQTLs for 183 and 83 *cis*-genes, respectively. This implies that these disease loci confer risk of T2D, via the *cis*-regulation of the expression levels in tissue relevant to T2D for a large number (266 in total) of neighbouring genes. This study identifies a large number of disease loci at regulatory hotspots and replicates them in both European and African-American populations, with 84% (93/111) of the additional loci being cosmopolitan. This replication was made possible by analyses that make use of, rather than being confounded by, the fine-scale differences in LD between these two populations, where causal locations and also eQTLs are estimated on an LDU map, avoiding the ambivalence of interpreting individual GWAS SNPs. Interestingly, recent results in the literature support our conclusion that cosmopolitan loci are more widespread than previously thought. For example, it was not until recently that the most established bona-fide *TCF7L2* locus for T2D in Europeans was also confirmed in African ancestry groups in an extensive study that included 17 African-American GWA samples⁷. This is a locus that was identified in the present study, which included only one African-American sample.

The T2D associated common genetic variation in *TCF7L2* is well established, but the mechanism by which risk of disease is conferred remains elusive. Our refined localization

of this locus reveals that this is a regulatory site for the distant nuclear-encoded mitochondrial gene, *GPAM*, and identifies additional candidate causal variants *GPAM* is interesting as it is a key rate-limiting enzyme in lipogenesis and highly expressed in liver and adipose tissue. Nuclear-encoded mitochondrial genes are of particular interest in relation to T2D, since mitochondrial function has been demonstrated to impact upon a myriad of molecular and cellular functional processes implicated in T2D²⁴⁻²⁶. However, to date human genetic association studies have identified few, if any, nuclear-encoded mitochondrial genes that directly confer risk of T2D in its common form. In this study we have identified at least 11 further nuclear-encoded mitochondria genes, which are regulated by eQTLs that also appear to confer risk of T2D. This indicates that one of the molecular mechanisms that contribute to inherited risk of T2D is mitochondrial dysfunction in relation to energy metabolism. These findings are also supported by an independent study design that utilises transcriptome and proteome data to reconstruct metabolic pathways in myocytes and identify the same mitochondrial pathways implicated in our study for adipose tissue (namely, fatty acid beta-oxidation, Krebs cycle, pyruvate metabolism and branched-chain amino acid (valine, leucine, and isoleucine) metabolism)²⁷.

Recent large scale whole genome and exome association studies²⁸ have empirically questioned any major role for coding variants in the aetiology of T2D and therefore make regulatory loci such as the ones highlighted in this study, all the more important to investigate. We believe that the targeted re-sequencing of informative refined regions using case/control data has the power to dissect the genetic epidemiology of T2D. While imputation methods can successfully infer missing genotypes for most genomic regions

using population data as the reference data, ironically it appears that imputation methods are likely to fail to impute or to make correct inferences where it matters most (e.g. at disease loci with allelic spectra that differ from the general population). This important point requires further investigation.

Chromatin analyses and targeted re-sequencing of these refined regions can be used to identify potential causal variant locations. The two identified signals (*ACTL7B* and *KCNK3*), which we have investigated lends support to this approach. A cosmopolitan disease location interval that includes *KCNK3* was observed to be a hotspot for the regulation of six neighboring genes, with *OTOF* of particular interest because of its known association with hearing loss (autosomal recessive forms of deafness²⁹). According to the NIDDK, the prevalence of low- or mid-frequency hearing impairment among diabetics is three times that of non-diabetics (28% compared with 9%)³⁰ with the potential mechanism operating via microvascular and neural damage due to long-term hyperglycaemia³¹. Interestingly, adipose gene expression for *OTOF* has also been previously shown to be associated with BMI in the morbidly obese²⁹ providing further evidence of a functional role through a regulatory mechanism. Targeted re-sequencing within the *KCNK3* location interval identified candidate causal variants with large effect sizes. As with the *TCF7L2* locus, the T2D and eQTL locations were found to reside in pancreatic islet enhancer and FOXA2 transcription factor-binding sites. Studies have shown that dysregulation of islet enhancers is relevant to the underlying mechanisms of T2D²² and a recent examination of some of the previously found T2D loci have been found to overlap with FOXA2-bound sites³².

The cosmopolitan T2D location interval near *ACTL7B* overlapped with chromatin peaks for CD14⁺ monocytes and included an eQTL for *KLF4* and *EPB41L4B*. *KLF4* is highly expressed in CD14⁺ monocytes and belongs to the Krüppel-like factor (KLF) family that consists of transcription factors that can activate or repress different genes involved in processes such as differentiation, development and cell cycle progression, with several of these proteins implicated in glucose homeostasis³³. *KLF4* is also used experimentally to induce pluripotent cells that can differentiate into insulin-producing cells³⁴. *EPB41L4B* codes for an erythrocyte membrane protein (EMP) with greatly increased EMP glycosylation observed in T2D subjects³⁵ with likely clinical implications³⁶. It is recognized clinically that both obesity and T2D are associated with a state of abnormal inflammatory response. Here we show that the T2D variants and eQTL locations for *KLF4* and *EPB41L4B* reside in regions with chromatin modifications mainly observed in CD14⁺ monocytes. Monocytes play a pivotal role in innate immunity and are involved in metabolic regulation³⁷. It has been shown that unbalanced proinflammatory/anti-inflammatory markers of CD14⁺ cells is associated with metabolic disorder in obese T2D individuals³⁸. *KLF4* is a critical regulator of monocyte differentiation³⁹ and *EPB41L4B* expression in subcutaneous and omental adipose is strongly associated with BMI in morbidly obese individuals²⁰. Therefore, these T2D intragenic variants and the regulated *cis*-genes (*KLF4* and *EPB41L4B*) are likely to be involved in an inflammatory pathway for obesity and T2D.

The complex causal chain between a gene and its effect on susceptibility cannot be unravelled until we have a full understanding of the regulatory genetic architecture that

underpins T2D, and until the causal changes have been localized in the DNA sequence⁴⁰. Our results show that disease-associated loci in different populations, gene expression and cell-specific regulatory annotation can be effectively integrated by localizing these effects on high-resolution linkage disequilibrium maps. By exploiting these maps to refine causal location estimates, we have identified a genomic catalogue of cosmopolitan and European disease loci with correspondingly important clinical implications that provides important molecular insights and opportunities to understand the molecular basis of this devastating common disease.

Supplemental Information

Supplemental Information include methods two figures and two tables.

Acknowledgements

We would like to thank the WTCCC, UK, for making the WTCCC T2D genomic data available. A full list of the investigators who contributed to the generation of the data is available from www.wtccc.org.uk. We are grateful to the NIDDK, USA, for making the AA T2D phenotype and genomic data available to us. The NIDDK whole genome association search for T2D genes in African-Americans was conducted by Donald Bowden, Center for Human Genomics, Center for Diabetes Research, Wake Forest University School of Medicine, Winston-Salem, USA, with support from the NIDDK. The datasets used were obtained from the database of Genotypes and Phenotypes (dbGaP) at accession number phs000140. This manuscript was not prepared in collaboration with the labs of any of the investigators responsible for generating the data, and does not necessarily reflect the views or opinions of these investigators. TA would like to acknowledge the Medical Research Council UK [Investigator Award 91993] for supporting his work. All authors are grateful to Professor Dallas Swallow (UCL) for her valuable comments on the manuscript, Professor Philippe Froguel (Imperial College, CNRS 8199, EGID 59045) for generously supplying us with European DNA samples for the NGS pilot work and Aminah Ali (UCL) for her valuable contributions to processing the NGS data. NM would like to acknowledge Newton E. Morton (Southampton) for the previous body of work on LDU maps.

Conflicts of interest

No conflict of interest to declare.

Table 1. Identified cosmopolitan T2D susceptibility loci and their regulatory role of neighbouring gene expression

Table 2. Identified European-specific T2D susceptibility loci and their regulatory role of neighbouring gene expression

Table 1. Identified cosmopolitan T2D susceptibility loci and their regulatory role of neighbouring gene expression

^aT2D associated intervals in kb (<100) that harbour T2D susceptibility loci in both populations, the minimum distance is provided for signals 1-5; ^bLocation estimates for the European (E) GWAS; ^cLocation estimates for the African-American (A) GWAS; ^dLocation estimates for the Metaboship European (E) samples, signals with low SNP coverage ‘-’ were not meta-analysed; ^eGenes in bold denote the intragenic localization and genes with ‘+’ for self-regulatory; ^fNumber of *cis*-genes regulated by the eQTL; ^gList of *cis*-genes associated with eQTLs that co-located within <50kb of the T2D locations, *cis*-genes with ‘**’ have previously shown evidence of association between Body Mass Index in morbidly obese and adipose/liver expression profiles²⁰; ^hDistance in kb (<50) between eQTL and T2D locations, the minimum is given when more than one *cis*-gene is implicated.

Signal	Chr.	Meta P-value	Distance between locations ^a	T2D location GWAS-E ^b	T2D location GWAS-A ^c	T2D location metabo-E ^d	Nearest gene to T2D locations ^e	no. of <i>cis</i> -genes ^f	eQTL associated <i>cis</i> -genes ^g	eQTL distance from T2D ^h
1	4p	1.73E-56	1	44797	44857	44858	-	0	-	-
2	6q	5.28E-10	4	72479	72509	72505	-	1	<i>FAM135A</i>	1
3	13q	2.14E-35	28	109848	109805	109833	COL4A2	1	<i>ANKRD10</i>	20
4	17q	2.80E-12	7	65769	65762	65769	KCNJ2	1	<i>MAP2K6</i>	37
5	20q	1.83E-06	77	44104	44181	44104	SLC12A5, CD40*	2	<i>CD40, CDH22</i>	17
6	1p	2.48E-06	41	82826	82826	-	-	1	<i>LPHN2*</i>	8
7	1p	5.20E-07	73	84451	84524	-	PRKACB*, SAMD13*	3	<i>PRKACB, SAMD13, C1orf52</i>	6
8	1p	1.79E-11	94	106441	106535	-	-	1	<i>PRMT6</i>	3
9	1q	5.03E-14	8	207662	207670	-	MIR205HG	0	-	-
10	1q	3.40E-09	3	232337	232340	-	SLC35F3	0	-	-
11	1q	1.07E-07	52	234896	234948	-	ACTN2	3	<i>TBCE*, B3GALNT2, ARID4B</i>	23
12	1q	6.33E-07	49	243993	244042	-	SMYD3	0	-	-
13	2p	4.57E-07	95	12139	12044	-	MIR3681HG	0	-	-
14	2p	2.62E-15	89	45025	44936	-	SIX3, CAMKMT	3	<i>PRKCE*, DYNC2LI1, ABCG8</i>	27
15	2q	2.61E-09	89	139530	139527	-	-	0	-	-
16	3p	4.05E-07	42	7503	7461	-	GRM7	1	<i>RAD18</i>	17
17	3p	1.20E-10	0	38370	38369	ns	XYLB	0	-	-
18	3p	5.10E-11	95	41078	41173	ns	CTNNB1	2	<i>CTNNB1*, ZNF621</i>	1
19	3p	4.22E-23	13	47556	47569	ns	CSPG5	4	<i>IP6K2 (IHPK2)*, KIF9, TESSP5, P4HTM</i>	3
20	3p	8.39E-06	20	54986	54965	-	CACNA2D3	0	-	-
21	3p	1.13E-13	59	67827	67768	-	SUCLG2	0	-	-
22	3p	6.67E-10	9	87317	87327	ns	CHMP2B	0	-	-
23	3q	7.80E-06	18	122056	122038	-	BC032918	2	<i>CD86*, ILDR1</i>	4
24	3q	5.39E-08	49	184743	184694	-	KLHL6	3	<i>AP2M1, ABCF3, MAGEF1</i>	0
25	4q	1.87E-11	24	53132	53108	ns	USP46*	1	<i>USP46</i>	2
26	4q	2.68E-07	6	92162	92168	-	CCSER1	2	<i>HSD17B13, PDHA2</i>	0
27	4q	5.24E-13	56	96319	96376	-	UNC5C	1	<i>PDHA2</i>	2
28	4q	4.02E-13	3	102095	102098	-	PPP3CA	0	-	-
29	4q	1.50E-06	74	148449	148375	>100kb	-	1	<i>EDNRA</i>	1
30	5q	8.84E-06	44	52127	52083	-	PELO	1	<i>ITGA1</i>	20
31	5q	1.56E-08	14	59263	59277	-	PDE4D*	1	<i>PDE4D*</i>	38
32	5q	2.81E-06	77	97282	97359	-	-	0	-	-
33	6p	1.00E-07	86	40514	40429	-	LRFN2, BC132805	2	<i>KCNK5, UNC5CL*</i>	0
34	6p	1.30E-15	72	44790	44718	-	BX647715	1	<i>PTK7</i>	4
35	6q	3.04E-07	5	168842	168837	-	SMOC2	3	<i>MLLT4*, CCR6, C6orf122</i>	1
36	7p	6.93E-08	85	24390	24305	-	NPY	2	<i>CCDC126, OSBPL3</i>	35
37	7p	1.49E-08	4	35510	35514	-	HERPUD2	1	<i>AAA1</i>	34
38	7p	5.97E-06	75	37471	37396	-	ELMO1*	2	<i>ELMO1, GPR141</i>	30
39	7q	4.00E-06	77	82225	82149	-	PCLO	1	<i>HGF*</i>	26
40	7q	4.78E-12	62	132516	132454	-	CHCHD3	0	-	-
41	7q	1.30E-09	73	133716	133789	-	SLC35B4, AKR1B1	0	-	-
42	7q	4.44E-10	14	134336	134322	-	AGBL3	1	<i>TMEM140*</i>	0

43	7q	6.98E-14	75	141873	141798	-	TCRBV20S1, TCRB	4	<i>FAM131B*, ZYX, OR2A25, OR2F1</i>	0
44	8p	4.81E-08	93	14339	14246	-	SGCZ	2	<i>C8orf79, TUSC3</i>	11
45	8q	7.00E-08	87	70416	70503	-	SULF1	1	<i>PRDM14</i>	46
46	9q	6.46E-08	13	110613	110626	ns	ACTL7B	2	<i>EPB41L4B*, KLF4</i>	29
47	9q	8.64E-07	19	132799	132781	-	FIBCD1	4	<i>ABL1*, AIF1L, RAPGEF1* PRDM12</i>	23
48	10q	5.13E-10	11	44467	44456	>100kb	-	1	<i>ZNF22*</i>	32
49	10q	1.28E-06	8	57261	57268	-	-	1	<i>CDC2</i>	0
50	10q	9.29E-09	0	65408	65408	ns	CR622643	0	-	-
51	10q	8.37E-11	66	77817	77883	-	C10orf11+	2	<i>C10orf11, DUPD1</i>	1
52	11p	4.29E-09	5	22257	22262	-	ANO5	0	-	-
53	11p	5.53E-13	88	32453	32364	-	WT1+	4	<i>PRRG4*, FBXO3*, ELP4, WT1</i>	14
54	11q	4.12E-08	0	57558	57558	ns	OR9Q1	1	<i>MPEG1</i>	33
55	11q	1.11E-09	21	59295	59315	-	STX3	0	-	-
56	12p	1.40E-07	31	25404	25373	-	KRAS	1	<i>SSPN</i>	0
57	12p	8.75E-07	6	29568	29574	-	TMTC1	0	-	-
58	12q	3.45E-06	91	57035	57127	ns	-	2	<i>SLC26A10, MBD6</i>	1
59	12q	8.78E-06	34	61602	61636	-	PPMIH	0	-	-
60	12q	2.45E-06	62	98425	98363	-	ANKS1B	0	-	-
61	12q	1.45E-06	22	104931	104909	-	NUAK1	1	<i>MTERFD3</i>	0
62	13q	2.09E-07	85	26479	26564	-	USP12	0	-	-
63	13q	8.19E-06	40	47133	47173	-	-	0	-	-
64	13q	7.16E-14	13	65393	65380	-	MIR548X2	0	-	-
65	13q	1.10E-14	82	66885	66803	-	-	0	-	-
66	13q	5.74E-07	44	101207	101251	-	FGF14*	3	<i>TMTC4, PCCA, FGF14</i>	0
67	15q	1.13E-06	16	45938	45954	-	LINC01494	0	-	-
68	16p	2.90E-10	80	1700	1781	-	MAPK8IP3, IGFALS	7	<i>HAGH*, PGP*, TPSAB1*, FAHDI, GFER, GNPTG, PRR25</i>	0
69	16p	2.24E-06	32	12605	12636	-	SNX29	3	<i>CLEC16A*, SOCSI, LITAF</i>	10
70	16q	1.75E-26	4	70999	70995	>100kb	AK055364	1	<i>HYDIN</i>	2
71	16q	1.03E-11	20	77036	77016	-	WWOX	0	-	-
72	16q	5.52E-19	29	78435	78406	-	LOC101928248	2	<i>MAF*, WWOX</i>	11
73	17q	4.15E-07	47	34640	34593	>100kb	STAC2, CACNB1	4	<i>PLXDC1, CRKRS, ZBP2, KRT222</i>	6
74	18q	9.58E-10	0	36270	36271	-	-	0	-	-
75	18q	6.84E-06	72	74880	74809	-	SALL3	0	-	-
76	21q	3.09E-09	30	20521	20490	-	DYRK1A	0	-	-
77	21q	9.56E-08	61	27738	27677	-	MIR5009	0	-	-
78	21q	1.35E-10	39	34148	34109	-	ITSN	2	<i>C21orf66, TCP10L</i>	0
79	21q	1.53E-06	1	37635	37633	-	DYRK1A	1	<i>KCNJ6</i>	0
80	22q	7.29E-09	0	31376	31376	-	SYN3	1	<i>PISD</i>	12
81	2p	6.46E-06	7	ns	21294	21301	-	1	<i>SDC1</i>	33
82	2p	5.02E-09	0	>100kb	26774	26774	KCNK3	6	<i>OTOF*, GAREM2, CCDC121, ASXL2, DNMT3A, CENPA</i>	3
83	2q	1.02E-11	1	>100kb	135313	135313	ACMSD	0	-	-
84	2q	2.25E-11	0	ns	203732	203732	NBEAL1	0	-	-
85	4q	2.77E-09	8	>100kb	103404	103395	SLC39A8*	1	<i>SLC39A8</i>	0
86	6p	2.09E-13	60	ns	28525	28586	ZSCAN23, PX6	8	<i>ZKSCAN3, PGBD1*, MAS1L, OR2W1, OR11A1, HLA-F, IFITM4P, ZNF184</i>	6
87	8p	1.54E-18	44	>100kb	18194	18238	NAT1, NAT2	3	<i>PDGFRL*, CSGALNACT1, PCM1</i>	1
88	11p	1.86E-20	86	>100kb	8508	8594	STK33, TRIM66	0	-	-
89	12q	4.10E-16	44	>100kb	48574	48618	FAIM2*	1	<i>FAIM2</i>	10
90	15q	1.93E-07	77	ns	61133	61210	TPM1+, LACTB*	9	<i>TPM1, RPS27L*, DAPK2*, SNX1, LACTB, APH1B, HERC1, FAM96A, VPS13C</i>	1
91	17q	2.02E-06	86	>100kb	44633	44548	GNGT2*, BAGALNT2	3	<i>GNGT2, SAMD14*, HOXB3*</i>	19
92	17q	3.95E-08	85	>100kb	60951	60866	AXIN2*	1	<i>AXIN2</i>	38
93	20p	1.90E-19	31	>100kb	25718	25687	FAM182B	0	-	-

Table 2. Identified European-specific T2D susceptibility loci and their regulatory role of neighbouring gene expression

^aT2D associated intervals in kb (<100) that harbour T2D susceptibility loci in two European populations; ^bT2D location estimates for the European (E) GWAS;

^cThe African-American (A) GWAS yielded either significant but distant locations from the European T2D location (>100kb) or not significant 'ns' estimates;

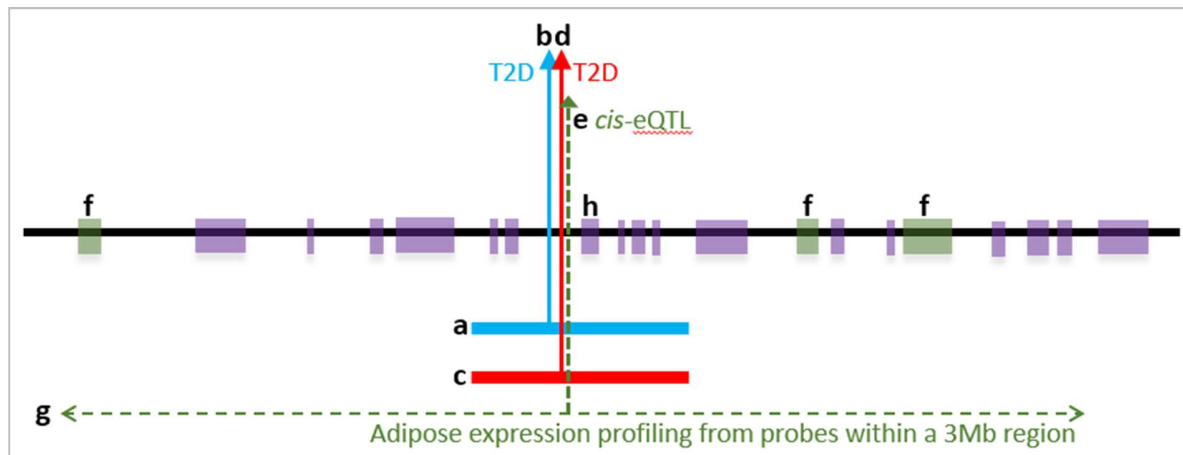
^dLocation estimates for the Metaboship European (E) samples that were within <100kb of the GWAS-E location; ^eGenes in bold denote the intragenic

localization and genes with '+' for self-regulatory genes; ^fNumber of cis-genes regulated by the eQTLs; ^gList of cis-genes associated with eQTLs that co-located within <50kb of the T2D locus, cis-genes with '*' have previously shown evidence of association between Body Mass Index for morbidly obese and

adipose/liver expression profiles²⁰; ^hDistance in kb (<50) between eQTL and T2D locations, the minimum is given when more than one cis-gene is implicated.

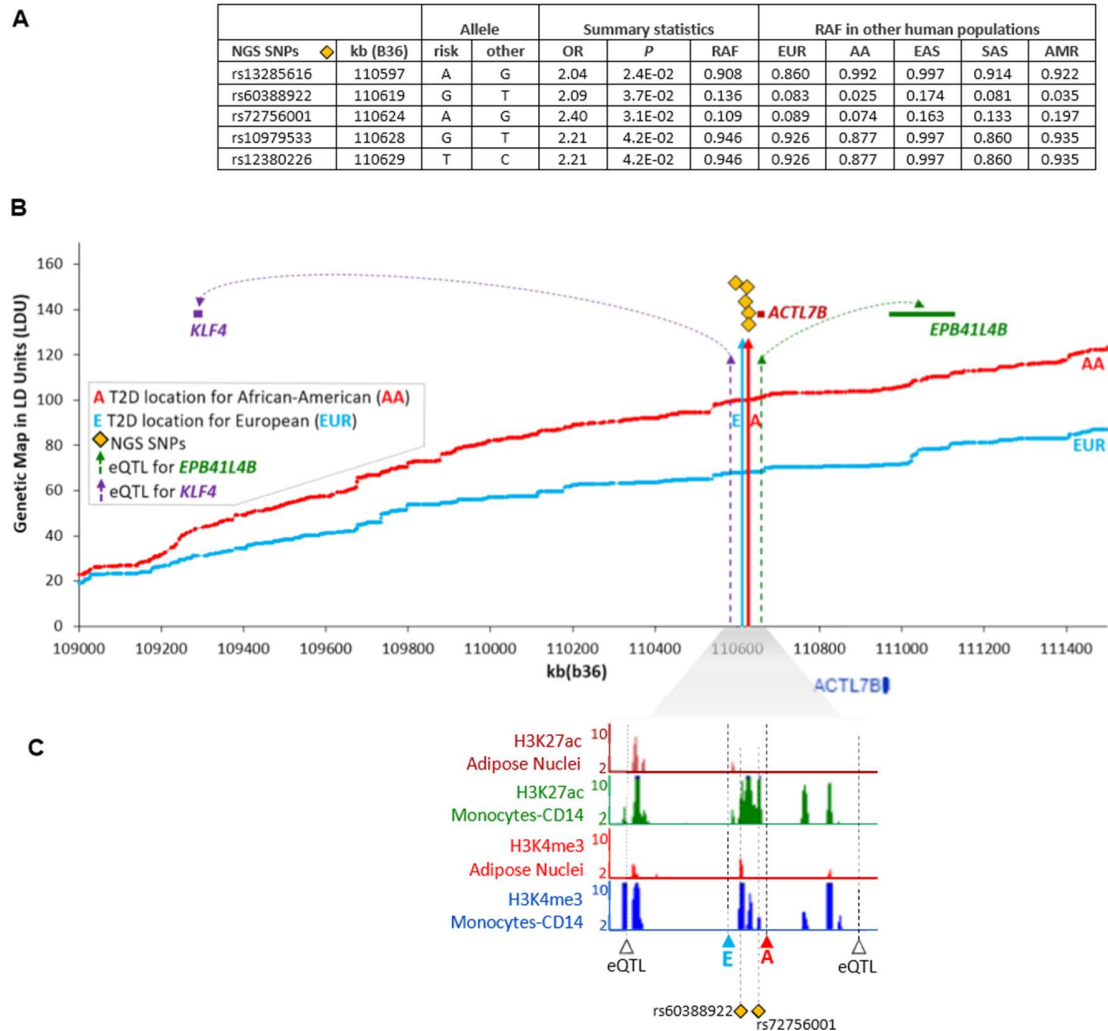
Signal	Chr.	Meta P-value	Distance of T2D locations ^a	T2D location GWAS-E ^b	T2D location GWAS-A ^c	T2D location metabo-E ^d	Nearest gene to T2D locations ^e	no. of cis-genes ^f	eQTL associated cis-genes ^g	eQTL distance from T2D ^h
94	1p	2.02E-07	3	25879	ns	25876	<i>MAN1C1</i>	2	<i>DHDDS, C1orf172</i>	0
95	1q	6.94E-12	21	228322	ns	228344	<i>GALNT2</i>	0	-	-
96	2p	4.11E-34	34	605	ns	639	<i>TMEM18</i>	0	-	-
97	2p	1.18E-07	46	40320	>100kb	40274	<i>SLC8A1-AS1</i>	4	<i>THUMP2, TMEM178, MORN2, DHX57</i>	0
98	3p	1.03E-09	5	53518	ns	53513	<i>CACNA1D</i>	0	-	-
99	3q	9.35E-07	7	133919	ns	133912	<i>ACAD11*</i>	8	<i>ACAD11, SLC02A1, RYK, NPHP3, ACKR4, SRPRB, CDV3, RAB6B</i>	0
100	4q	1.86E-22	66	104224	>100kb	104157	<i>BDH2, NHEDC1</i>	0	-	-
101	5q	2.62E-09	12	76449	ns	76461	<i>ZBED3</i>	1	<i>PDE8B*</i>	15
102	6p	2.64E-24	13	29662	ns	29674	<i>GABBR1</i>	7	<i>GNL1*, TRIM10, TRIM27, DDR1, TRIM40, TRIM15, ORI10C1</i>	9
103	6p	1.46E-28	6	31709	>100kb	31704	<i>BAT2, AIF1</i>	14	<i>AIF1*, TRIM39*, AGER, BAT4, CCHCR1, DOM3Z, EHMT2, HLA-DMB, HLA-DPA1, HSPA1B, LST1, TRIM10, NOTCH4, HLA-DRA</i>	0
104	6q	6.29E-56	0	118801	>100kb	118801	<i>SLC35F1</i>	0	-	-
105	6q	4.23E-17	37	127581	ns	127544	<i>RSPO3*</i>	2	<i>RSPO3, TRMT11</i>	1
106	10q	3.39E-24	40	104790	>100kb	104830	<i>CNNM2</i>	0	-	-
107	11p	2.50E-06	1	43836	ns	43836	<i>HSD17B12</i>	1	<i>HSD17B12</i>	1
108	11q	6.39E-06	21	65337	>100kb	65357	<i>OVL1, SNX32*</i>	4	<i>SNX32, MAJIN*, SNX15, EFEMP2</i>	9
109	12q	6.16E-06	4	54905	>100kb	54909	<i>OBFC2B*</i>	4	<i>OBFC2B, RGL1*, RPS26, STAT2</i>	0
110	12q	4.66E-08	3	111476	>100kb	111473	<i>PTPN11</i>	4	<i>ERP29, TMEM116, MAPKAPK5, NAPI</i>	20
111	17q	3.05E-09	51	25003	>100kb	25054	<i>SSH2</i>	1	<i>CORO6</i>	9

Figure 1. A schematic presentation of the functional genomic study design



^aThe LDU window of the European (EUR) genetic map; ^blocation of the causal variant for T2D estimated on the EUR map using a EUR GWAs; ^cthe African-American (AA) LDU genetic map; ^dlocation of the causal variant for T2D estimated on the AA map using an AA GWAs; ^elocation of the *cis*-eQTL for the three ^fassociated *cis*-gene that are implicated using adipose expression data^g from probes for genes within ± 1.5 Mb distance either side of the T2D locations^{bd}. In this example the nearest gene^h is not the implicated regulated gene.

Figure 2. Candidate causal variants at T2D locations in the *ACTL7B* region and their regulatory role

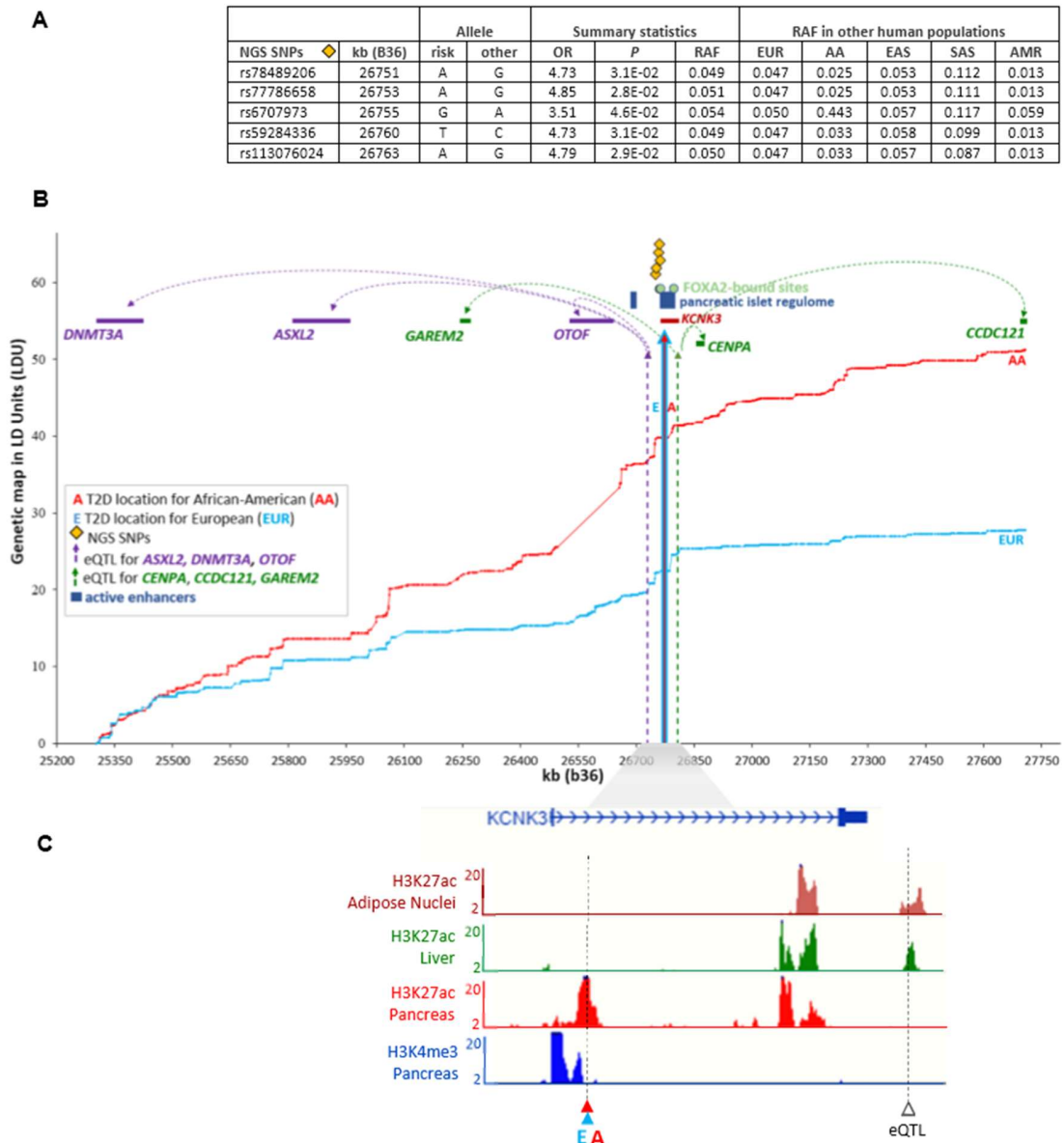


A: Identified T2D associated SNPs using targeted next generation sequencing (NGS) of the functional location estimates on the LDU genetic maps in Fig. 2B and their risk allele frequency (RAF) in Europeans (EUR), African-Americans (AA), East Asian (EAS), South Asian (SAS) and Mexican-Americans (AMR).

B: The two LDU genetic maps (Y-axis in LDU) for AA and EUR are plotted against the physical genomic region (X-axis in kb). Vertical solid line arrows represent the functional location estimates A and E that are associated with T2D in AA and EUR samples, respectively. The dotted line arrows are the locations of eQTLs.

C: $-\log_{10}$ P-values of cell type-specific chromatin profiles are plotted against the kb map. T2D, eQTL and NGS SNP locations overlap with the co-ordinates of the chromatin peaks.

Figure 3. Candidate causal variants at T2D locations in the *KCNK3* region and their regulatory role

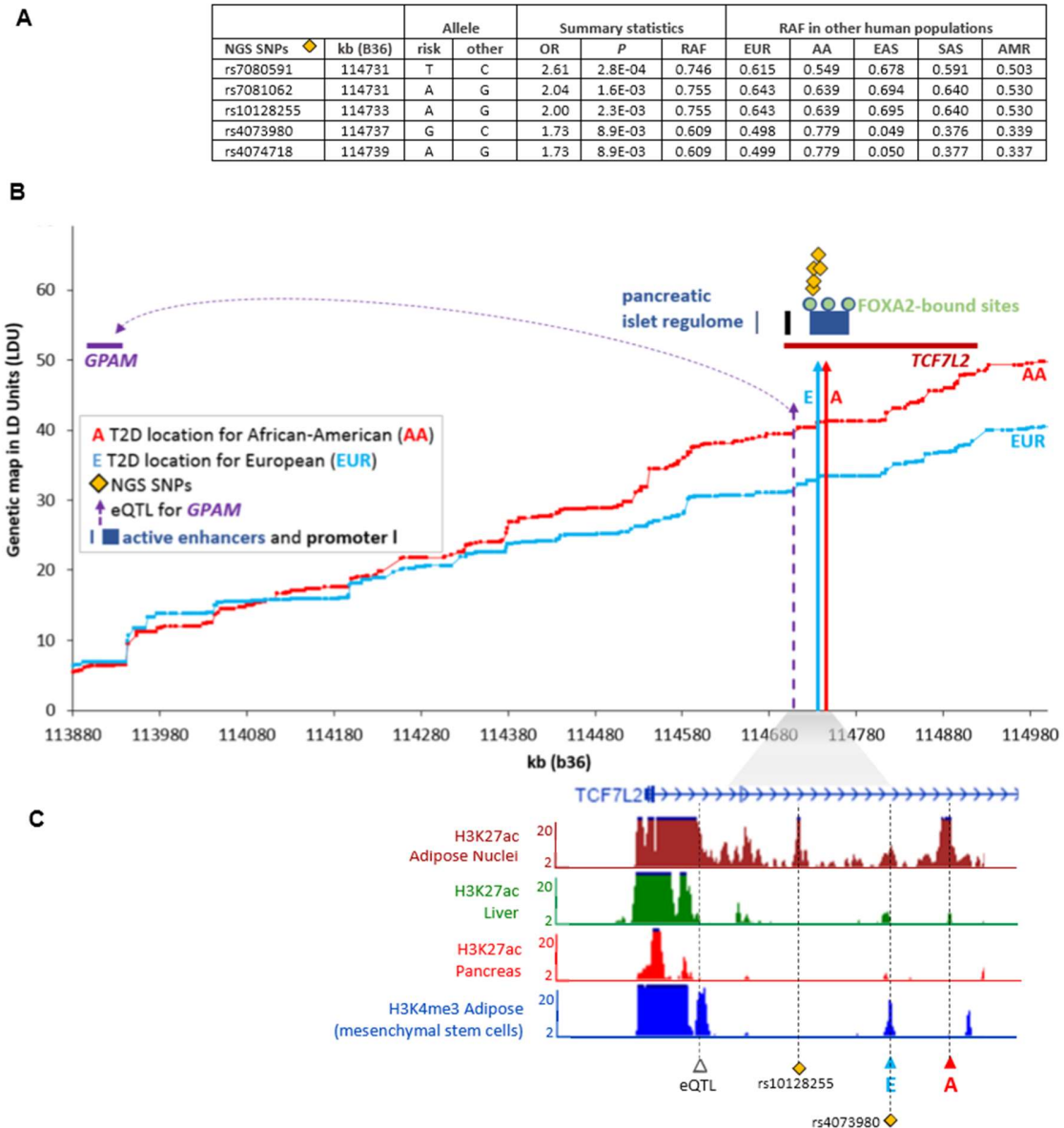


A: Identified T2D associated SNPs using targeted next generation sequencing (NGS) of the functional location estimates on the LDU genetic maps in Fig. 2B and their risk allele frequency (RAF) in Europeans (EUR), African-Americans (AA), East Asian (EAS), South Asian (SAS) and Mexican-Americans (AMR).

B: The two LDU genetic maps (Y-axis in LDU) for AA and EUR are plotted against the physical genomic region (X-axis in kb). Vertical solid line arrows represent the functional location estimates A and E that are associated with T2D in AA and EUR samples, respectively. The dotted line arrows are the locations of eQTLs.

C: $-\log_{10}$ P-values of cell type-specific chromatin profiles are plotted against the kb map. T2D and eQTL locations overlap with the co-ordinates of the chromatin peaks.

Figure 4. Candidate causal variants at T2D locations in the *TCF7L2* region and their regulatory role



A: Identified T2D associated SNPs using targeted next generation sequencing (NGS) of the functional location estimates on the LDU genetic maps in Fig. 2B and their risk allele frequency (RAF) in Europeans (EUR), African-Americans (AA), East Asian (EAS), South Asian (SAS) and Mexican-Americans (AMR).

B: The two LDU genetic maps (Y-axis in LDU) for AA and EUR are plotted against the physical genomic region (X-axis in kb). Vertical solid line arrows represent the functional location estimates A and E that are associated with T2D in AA and EUR samples, respectively. The dotted line arrow is the location of eQTL.

C: $-\log_{10}$ P-values of cell type-specific chromatin profiles are plotted against the kb map. T2D, eQTL and NGS SNP locations overlap with the co-ordinates of the chromatin peaks.

Web Resources

HapMap:

<ftp://ftp.ncbi.nlm.nih.gov/hapmap/>

Islet Regulome Browser

<http://gattaca.imppc.org/isletregulome/home>

MuTHER

<http://www.muther.ac.uk>

Online Mendelian Inheritance in Man:

<http://www.omim.org>

Roadmap Epigenetics Project

<http://www.roadmapepi genomics.org>

The 1000 Genomes Project

<http://www.internationalgenome.org>

References

1. Altshuler, D., and Daly, M. (2007). Guilt beyond a reasonable doubt. *Nat Genet* 39, 813-815.
2. Lebovitz, H.E. (1999). Type 2 diabetes: an overview. *Clinical chemistry* 45, 1339-1345.
3. Mahajan, A., Go, M.J., Zhang, W., Below, J.E., et al.; DIAbetes Genetics Replication And Meta-analysis (DIAGRAM) Consortium; Asian Genetic Epidemiology Network Type 2 Diabetes (AGEN-T2D) Consortium; South Asian Type 2 Diabetes (SAT2D) Consortium; Mexican American Type 2 Diabetes (MAT2D) Consortium; Type 2 Diabetes Genetic Exploration by Nex-generation sequencing in muylti-Ethnic Samples (T2D-GENES) Consortium (2014). Genome-wide trans-ancestry meta-analysis provides insight into the genetic architecture of type 2 diabetes susceptibility. *Nat Genet* 46, 234-244.
4. Morris, A.P., Voight, B.F., Teslovich, T.M., Ferreira, T., Segre, A.V., Steinthorsdottir, V., Strawbridge, R.J., Khan, H., Grallert, H., Mahajan, A., et al. (2012). Large-scale association analysis provides insights into the genetic architecture and pathophysiology of type 2 diabetes. *Nat Genet*.
5. Li, Y.R., and Keating, B.J. (2014). Trans-ethnic genome-wide association studies: advantages and challenges of mapping in diverse populations. *Genome medicine* 6, 91.
6. Asimit, J.L., Hatzikotoulas, K., McCarthy, M., Morris, A.P., and Zeggini, E. (2016). Trans-ethnic study design approaches for fine-mapping. *European journal of human genetics : EJHG*.
7. Ng, M.C., Shriner, D., Chen, B.H., Li, J., Chen, W.M., Guo, X., Liu, J., Bielinski, S.J., Yanev, L.R., Nalls, M.A., et al. (2014). Meta-analysis of genome-wide association studies in African Americans provides insights into the genetic architecture of type 2 diabetes. *PLoS Genet* 10, e1004517.
8. Direk, K., Lau, W., Small, K.S., Maniatis, N., and Andrew, T. (2014). ABCC5 transporter is a novel type 2 diabetes susceptibility gene in European and African American populations. *Ann Hum Genet* 78, 333-344.
9. Elding, H., Lau, W., Swallow, D.M., and Maniatis, N. (2013). Refinement in localization and identification of gene regions associated with Crohn disease. *Am J Hum Genet* 92, 107-113.
10. Zhang, X., Bailey, S.D., and Lupien, M. (2014). Laying a solid foundation for Manhattan--'setting the functional basis for the post-GWAS era'. *Trends Genet* 30, 140-149.
11. Wellcome Trust Case Control Consortium (2007). Genome-wide association study of 14,000 cases of seven common diseases and 3,000 shared controls. *Nature* 447, 661-678.
12. Voight, B.F., Kang, H.M., Ding, J., Palmer, C.D., Sidore, C., Chines, P.S., Burt, N.P., Fuchsberger, C., Li, Y., Erdmann, J., et al. (2012). The metabochip, a custom genotyping array for genetic studies of metabolic, cardiovascular, and anthropometric traits. *PLoS Genet* 8, e1002793.
13. Palmer, N.D., McDonough, C.W., Hicks, P.J., Roh, B.H., Wing, M.R., An, S.S., Hester, J.M., Cooke, J.N., Bostrom, M.A., Rudock, M.E., et al. (2012). A genome-wide association search for type 2 diabetes genes in African Americans. *PLoS One* 7, e29202.
14. Maniatis, N., Collins, A., and Morton, N.E. (2007). Effects of single SNPs, haplotypes, and whole-genome LD maps on accuracy of association mapping. *Genet Epidemiol* 31, 179-188.
15. Maniatis, N., Collins, A., Gibson, J., Zhang, W., Tapper, W., and Morton, N.E. (2004). Positional cloning by linkage disequilibrium. *Am J Hum Genet* 74, 846-855.
16. Maniatis, N., Collins, A., Xu, C.F., McCarthy, L.C., Hewett, D.R., Tapper, W., Ennis, S., Ke, X., and Morton, N.E. (2002). The first linkage disequilibrium (LD) maps: delineation of hot and cold blocks by diplotype analysis. *Proc Natl Acad Sci U S A* 99, 2228-2233.

17. Grundberg, E., Small, K.S., Hedman, A.K., Nica, A.C., Buil, A., Keildson, S., Bell, J.T., Yang, T.P., Meduri, E., Barrett, A., et al. (2012). Mapping cis- and trans-regulatory effects across multiple tissues in twins. *Nat Genet* 44, 1084-1089.
18. Vionnet, N., Hani, E.H., Dupont, S., Gallina, S., Francke, S., Dotte, S., De Matos, F., Durand, E., Lepretre, F., Lecoeur, C., et al. (2000). Genomewide search for type 2 diabetes-susceptibility genes in French whites: evidence for a novel susceptibility locus for early-onset diabetes on chromosome 3q27-qter and independent replication of a type 2-diabetes locus on chromosome 1q21-q24. *Am J Hum Genet* 67, 1470-1480.
19. Meyre, D., Lecoeur, C., Delplanque, J., Francke, S., Vatin, V., Durand, E., Weill, J., Dina, C., and Froguel, P. (2004). A genome-wide scan for childhood obesity-associated traits in French families shows significant linkage on chromosome 6q22.31-q23.2. *Diabetes* 53, 803-811.
20. Greenawalt, D.M., Dobrin, R., Chudin, E., Hatoum, I.J., Suver, C., Beaulaurier, J., Zhang, B., Castro, V., Zhu, J., Sieberts, S.K., et al. (2011). A survey of the genetics of stomach, liver, and adipose gene expression from a morbidly obese cohort. *Genome research* 21, 1008-1016.
21. Consortium, E.P. (2011). A user's guide to the encyclopedia of DNA elements (ENCODE). *PLoS biology* 9, e1001046.
22. Pasquali, L., Gaulton, K.J., Rodriguez-Segui, S.A., Mularoni, L., Miguel-Escalada, I., Akerman, I., Tena, J.J., Moran, I., Gomez-Marin, C., van de Bunt, M., et al. (2014). Pancreatic islet enhancer clusters enriched in type 2 diabetes risk-associated variants. *Nat Genet* 46, 136-143.
23. Trynka, G., Sandor, C., Han, B., Xu, H., Stranger, B.E., Liu, X.S., and Raychaudhuri, S. (2013). Chromatin marks identify critical cell types for fine mapping complex trait variants. *Nat Genet* 45, 124-130.
24. Lowell, B.B., and Shulman, G.I. (2005). Mitochondrial dysfunction and type 2 diabetes. *Science* 307, 384-387.
25. Mootha, V.K., Lindgren, C.M., Eriksson, K.F., Subramanian, A., Sihag, S., Lehar, J., Puigserver, P., Carlsson, E., Ridderstrale, M., Laurila, E., et al. (2003). PGC-1alpha-responsive genes involved in oxidative phosphorylation are coordinately downregulated in human diabetes. *Nat Genet* 34, 267-273.
26. Patti, M.E., and Corvera, S. (2010). The role of mitochondria in the pathogenesis of type 2 diabetes. *Endocr Rev* 31, 364-395.
27. Varemo, L., Scheele, C., Broholm, C., Mardinoglu, A., Kampf, C., Asplund, A., Nookaew, I., Uhlen, M., Pedersen, B.K., and Nielsen, J. (2015). Proteome- and transcriptome-driven reconstruction of the human myocyte metabolic network and its use for identification of markers for diabetes. *Cell reports* 11, 921-933.
28. Fuchsberger, C., Flannick, J., Teslovich, T.M., Mahajan, A., Agarwala, V., Gaulton, K.J., Ma, C., Fontanillas, P., Moutsianas, L., McCarthy, D.J., et al. (2016). The genetic architecture of type 2 diabetes. *Nature* 536, 41-47.
29. Duman, D., and Tekin, M. (2012). Autosomal recessive nonsyndromic deafness genes: a review. *Frontiers in bioscience* 17, 2213-2236.
30. Bainbridge, K.E., Hoffman, H.J., and Cowie, C.C. (2008). Diabetes and hearing impairment in the United States: audiometric evidence from the National Health and Nutrition Examination Survey, 1999 to 2004. *Annals of internal medicine* 149, 1-10.
31. Bainbridge, K.E., Cheng, Y.J., and Cowie, C.C. (2010). Potential mediators of diabetes-related hearing impairment in the U.S. population: National Health and Nutrition Examination Survey 1999-2004. *Diabetes Care* 33, 811-816.
32. Gaulton, K.J., Ferreira, T., Lee, Y., Raimondo, A., Magi, R., Reschen, M.E., Mahajan, A., Locke, A., William Rayner, N., Robertson, N., et al. (2015). Genetic fine mapping and

- genomic annotation defines causal mechanisms at type 2 diabetes susceptibility loci. *Nat Genet* 47, 1415-1425.
33. Gray, S., Feinberg, M.W., Hull, S., Kuo, C.T., Watanabe, M., Sen-Banerjee, S., DePina, A., Haspel, R., and Jain, M.K. (2002). The Kruppel-like factor KLF15 regulates the insulin-sensitive glucose transporter GLUT4. *The Journal of biological chemistry* 277, 34322-34328.
 34. Noguchi, H. (2009). Recent advances in stem cell research for the treatment of diabetes. *World journal of stem cells* 1, 36-42.
 35. Yamaguchi, M., Nakamura, N., Nakano, K., Kitagawa, Y., Shigeta, H., Hasegawa, G., Ienaga, K., Nakamura, K., Nakazawa, Y., Fukui, I., et al. (1998). Immunochemical quantification of crossline as a fluorescent advanced glycation endproduct in erythrocyte membrane proteins from diabetic patients with or without retinopathy. *Diabetic medicine : a journal of the British Diabetic Association* 15, 458-462.
 36. Adewoye, E.O., Akinlade, K.S., and Olorunsogo, O.O. (2001). Erythrocyte membrane protein alteration in diabetics. *East African medical journal* 78, 438-440.
 37. Fernandez-Real, J.M., and Pickup, J.C. (2008). Innate immunity, insulin resistance and type 2 diabetes. *Trends in endocrinology and metabolism: TEM* 19, 10-16.
 38. Satoh, N., Shimatsu, A., Himeno, A., Sasaki, Y., Yamakage, H., Yamada, K., Suganami, T., and Ogawa, Y. (2010). Unbalanced M1/M2 phenotype of peripheral blood monocytes in obese diabetic patients: effect of pioglitazone. *Diabetes Care* 33, e7.
 39. Feinberg, M.W., Wara, A.K., Cao, Z., Lebedeva, M.A., Rosenbauer, F., Iwasaki, H., Hirai, H., Katz, J.P., Haspel, R.L., Gray, S., et al. (2007). The Kruppel-like factor KLF4 is a critical regulator of monocyte differentiation. *The EMBO journal* 26, 4138-4148.
 40. Morton, N.E. (2005). Linkage disequilibrium maps and association mapping. *The Journal of clinical investigation* 115, 1425-1430.

